

# Investigation of the effects of free-stream turbulence on wind-induced responses of tall building by Large Eddy Simulation

Q.S. Li\*, G. Hu and Bo-wen Yan

*Department of Civil and Architectural Engineering, City University of Hong Kong, Hong Kong*

*(Received October 8, 2012, Revised January 3, 2014, Accepted January 12, 2014)*

**Abstract.** In this study, a square rectangular tall building is considered to investigate the effects of turbulence integral length scale and turbulence intensity on the along-wind responses, across-wind responses and torsional responses of the tall building by Large Eddy Simulation (LES). A recently proposed inflow turbulence generator called the discretizing and synthesizing random flow generation (DSRFG) approach is applied to simulate turbulent flow fields. It has been proved that the approach is able to generate a fluctuating turbulent flow field satisfying any given spectrum, desired turbulence intensity and wind speed profiles. Five profiles of turbulence integral length scale and turbulence intensity are respectively generated for the inflow fields by the DSRFG approach for investigating the effects of turbulence integral length scale and turbulence intensity on the wind-induced responses of the tall building. The computational results indicate that turbulence integral length scale does not have significant effect on the along-wind (displacement, velocity and acceleration) responses, across-wind displacement and velocity responses, while the across-wind acceleration and torsional responses vary without a clear rule with the parameter. On the other hand, the along-wind, across-wind and torsional responses increase with the growth of turbulence intensity.

**Keywords:** turbulence integral length scale; turbulence intensity; tall building; wind-induced response; CFD; LES

## 1. Introduction

Wind flow in the atmospheric boundary layer of the earth is highly turbulent. As a result, wind loads acting on buildings and structures are significantly influenced by turbulence characteristics. Turbulence integral length scale and turbulence intensity are two main parameters to describe the characteristics of natural wind. Turbulence integral length scale is the measurement of average size of the vortices. Turbulence intensity is the ratio of the standard deviation of fluctuating component to the mean value of wind velocity. It is related to the surface roughness of the ground.

In boundary layer wind tunnel testing, how to generate wind flows with arbitrary or desired values of turbulence integral length scale is a difficult problem. Varshney and Poddar (2011) conducted an investigation on controlling turbulence integral length scale values in a wind tunnel

---

\*Corresponding author, Professor, E-mail: [bcqqli@cityu.edu.hk](mailto:bcqqli@cityu.edu.hk)

and showed that the turbulence integral length scale can be controlled using different combinations of passive devices. However, it is difficult or impossible to generate wind flows with sufficiently large values of turbulence integral length scale in wind tunnels, even active devices are adopted. Compared with turbulence integral length scale, it is relatively easy to control turbulence intensity in wind tunnel tests.

During the past several decades, many researchers have conducted wind tunnel studies on the effects of turbulence on bluff bodies. Lee (1975a) reported that addition of turbulence to the flow causes an increase of base pressure and reduction of the drag of a two-dimensional square cylinder. His experiment showed the strength of the vortex shedding reduces as the growth of turbulence intensity. Lee (1975b) also investigated the effects of turbulence integral length scale on mean forces of square prisms and indicated that the mean drag is sensitive to the variation of turbulence integral length scale when it is around the body size. In addition, at high values of turbulence integral length scale the drag tends to a constant value greater than that at low values. Tieleman and Akins (1990) analyzed the effects of incident turbulence on pressure distributions on rectangular prisms. Their results showed that the pressure coefficients on the side and rear faces of the prisms vary primarily with the energy associated with the small scale turbulence in the incident flow. Laneville (1990) investigated the effect of turbulence scale ratio on pressure coefficients of two dimensional square cylinders and found that when turbulence scale ratio is larger than three, turbulence scale effect on mean drag is evident and the magnitude of this effect is about 12%. Nakamura (1993) pointed out that turbulence intensity and turbulence integral length scale have significant effects on pressure coefficients on bluff bodies. Saathoff and Melbourne (1987, 1989) concentrated their investigations on the effects of free-stream turbulence on the peak pressures on bluff bodies which are of primary concern in wind engineering. However, the largest ratio of turbulence integral length scale to model thickness in their studies was less than 2.0, which is smaller than the typical values of the turbulence scale ratio in the natural wind around buildings and structures. Thus, Li and Melbourne (1995, 1999a, b) conducted extensive experimental measurements over a larger range of turbulence scale ratio (0.3-30) to examine the effects of turbulence on surface pressures on various bluff bodies. However, all these previous studies were carried out in various uniform turbulent flows instead of in boundary layer flows. This is because for most boundary layer flows created in wind tunnels, turbulence intensity and turbulence integral length scale for a particular model usually increase or decrease together so that it is difficult to study their effects separately. But, for wind engineering applications, there is a need to investigate the effects of turbulence intensity and turbulence integral length scale on the wind effects on buildings and structures in boundary layer flows.

Besides the above mentioned studies carried out by wind tunnel tests, Computational Fluid Dynamics (CFD) becomes more and more attractive to study the wind effects on tall buildings (Swaddiwudhipong and Khan 2002, Huang *et al.* 2007, Tamura 2008, Tominaga *et al.* 2008, Braun and Awruch 2009, Tamura 2009, Huang *et al.* 2011, Yahyai 2011, Hang and Li 2012, Revuz *et al.* 2012) because of low cost and high-efficiency compared with wind tunnel testing. Theoretically speaking, CFD can overcome several drawbacks of wind tunnel testing, e.g., the limitations of generating wind flows with sufficiently large values of turbulence integral length scale and high Reynolds number such as those encountered in the atmospheric boundary layer wind flows. In addition, with the wind flows simulated by CFD, the effects of turbulence intensity and turbulence integral length scale on the wind effects on buildings and structures in boundary layer flows could be separately studied. However, to the authors' knowledge there have been very few studies conducted on the effect of turbulence on the wind-induced responses of tall buildings by CFD

techniques such as large eddy simulation (LES). One of the reasons may be attributed to that it is hard to generate wind flows exactly satisfying the target spectra and turbulence parameters for LES. In the present study, a new approach termed DSRFG (Huang *et al.* 2010), which has been proven to be able to generate real wind flow fields in the atmospheric boundary layer (Huang *et al.* 2010, Li *et al.* 2010, Lu *et al.* 2012), is adopted herein to generate inflow wind flows satisfying the target spectra and other turbulence parameters (turbulence intensity and turbulence integral length scale) to investigate the effects of free-stream turbulence on the wind-induced responses of a typical tall building.

## 2. Inflow turbulence generator for LES

### 2.1 Theory

Some previous studies revealed that most measured spectra of wind speed obey von Karman spectra (Li *et al.* 2004). In order to consider the effect of turbulence integral scale on the wind-induced responses of tall buildings, it is necessary to produce turbulent wind flows satisfying the von Karman spectra with any turbulence integral length scale. In this study, a newly developed inflow turbulence generation method, namely DSRFG, proposed by Huang *et al.* (2010), is employed to generate turbulent wind flow fields satisfying von Karman spectra. The detailed derivation of the DSRFG method is given by Huang *et al.* (2010), and a brief formulation of this method is presented below.

$$u(x, t) = \sum_{m=k_0}^{k_{\max}} u_m(x, t) = \sum_{m=k_0}^{k_{\max}} \sum_{n=1}^N [p^{m,n} \cos(\tilde{k}^{m,n} \cdot \tilde{x} + \omega_{m,n} t) + q^{m,n} \sin(\tilde{k}^{m,n} \cdot \tilde{x} + \omega_{m,n} t)] \quad (1)$$

where  $p^{m,n} = \zeta \times k^{m,n} / |\zeta \times k^{m,n}| \sqrt{a4E(k_m)/N}$ ,  $q^{m,n} = \xi \times k^{m,n} / |\xi \times k^{m,n}| \sqrt{(1-a)4E(k_m)/N}$ ,  $\tilde{x} = x / L_s$ ,  $\tilde{k}^{m,n} = k^{m,n} / k_0$ ,  $|k^{m,n}| = k_m$ ,  $\omega_{m,n} \in N(0, 2\pi k_m)$ ,  $\zeta$  and  $\xi$  are vector form of  $\zeta_i^n$  and  $\xi_i^n$ , respectively, and  $\zeta_i^n, \xi_i^n \in N(0,1)$ .  $k_m$  is wave number.  $L_s$  is turbulence integral length scale which is an important parameter used as the scaling factor for spatial correlation.  $a$  is a random number uniformly distributed between 0~1.  $N=100\sim 200$  (sampling number for each wave number  $k_m$ ) are found to be accurate enough and economical for most applications in wind engineering (Huang *et al.* 2010). The energy spectrum of turbulent wind velocity in each direction is fitted by the von Karman spectra, i.e.

$$S_u(f) = S_v(f) = S_w(f) = \frac{4(IU_{avg})^2(L/U_{avg})}{[1 + 70.8(fL/U_{avg})^2]^{5/6}} \quad (2)$$

So the 3D energy spectrum is given by

$$E(k) = E(kU_{avg}) = E(f) = \frac{3}{2} S_u(f) \quad (3)$$

By employing this approach, inflow fields with different turbulence characteristics such as turbulence intensities and turbulence integral length scales can be simulated. This method can be used to evaluate the effects of turbulence intensity and turbulence integral length scale on the wind-induced responses of tall buildings in boundary layer flows.

## 2.2 Validation and verification

In order to verify the validity of the DSRFG approach for generation of inflow wind fields, the LES for wind flows around a tall building is carried out using the DSRFG method. The wind tunnel testing for this tall building model was conducted by Reinhold (1977). The wind velocity and turbulence characteristics of incident wind flow in the wind tunnel testing are listed in Table 1 (Reinhold 1977).

Comparison of the longitudinal wind velocity spectra is made between the target von Karman spectrum and the spectrum generated by the DSRFG approach as shown in Fig. 1. Evidently, the spectrum determined by the DSRFG approach agrees well with the target von Karman spectrum. Fig. 2 shows the instantaneous velocity field at the inflow boundary generated by the DSRFG approach. A number of eddies are produced near the inflow boundary, while the velocity increases with height. Comparison of the mean velocity magnitude is shown in Fig. 3 in which the distributions of the mean velocity magnitude are mostly consistent with those simulated by Huang *et al.* (2010).

Figs. 4- 6 show comparisons of the normalized power spectral density functions of  $F_x$ ,  $F_y$  and  $M$  between the numerical results of this study and those in the literature including the experimental results by Reinhold (1977) and the predictions by Huang *et al.* (2010). For the along-wind force spectra and torsional moment spectra, the results of the present study agree well with the experimental results and the numerical results of Huang *et al.* (2010). However, the magnitudes of the across-wind force spectrum of this study are lower than those in the literature in low-frequency range but are higher in high-frequency range. Basically, the predictions of the wind forces and torsional moment obtained in this study are in good agreement with the experimental data and the numerical results of Huang *et al.* (2010), thus verifying the accuracy of the adopted inflow field generation method and the LES for the evaluation of wind effects on tall buildings.

Table 1 Inflow wind characteristics in the wind tunnel testing

Elevation(m)	Velocity(m/s)	Turbulence intensity (%)	Turbulence length scale (m)	Reynolds numbers
0.1016	10.1	27.71	0.2211	59000
0.2032	13.0	23.13	0.2766	75000
0.3048	15.1	18.12	0.3048	88000
0.4064	16.8	13.69	0.3052	98000
0.5080	18.3	10.25	0.2740	110000
0.6096	19.5	8.13	0.2345	110000

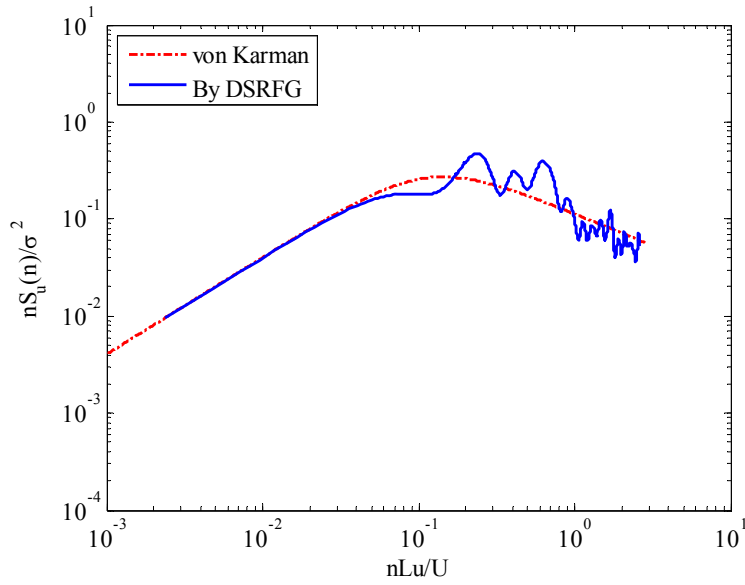


Fig. 1 Comparison of the wind velocity spectrum by the DSRFG and von Karman spectrum

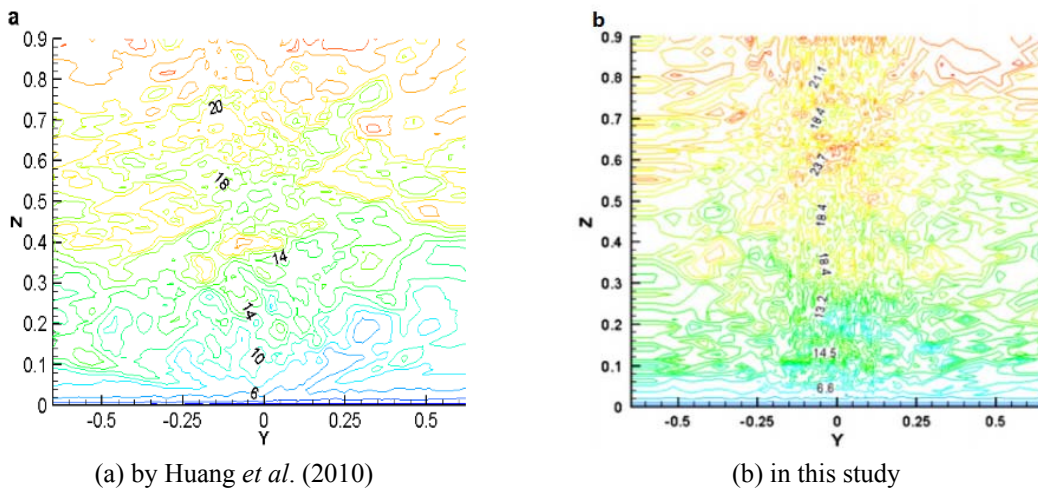


Fig. 2 Instantaneous velocity field at the inflow boundary generated by the DSRFG approach

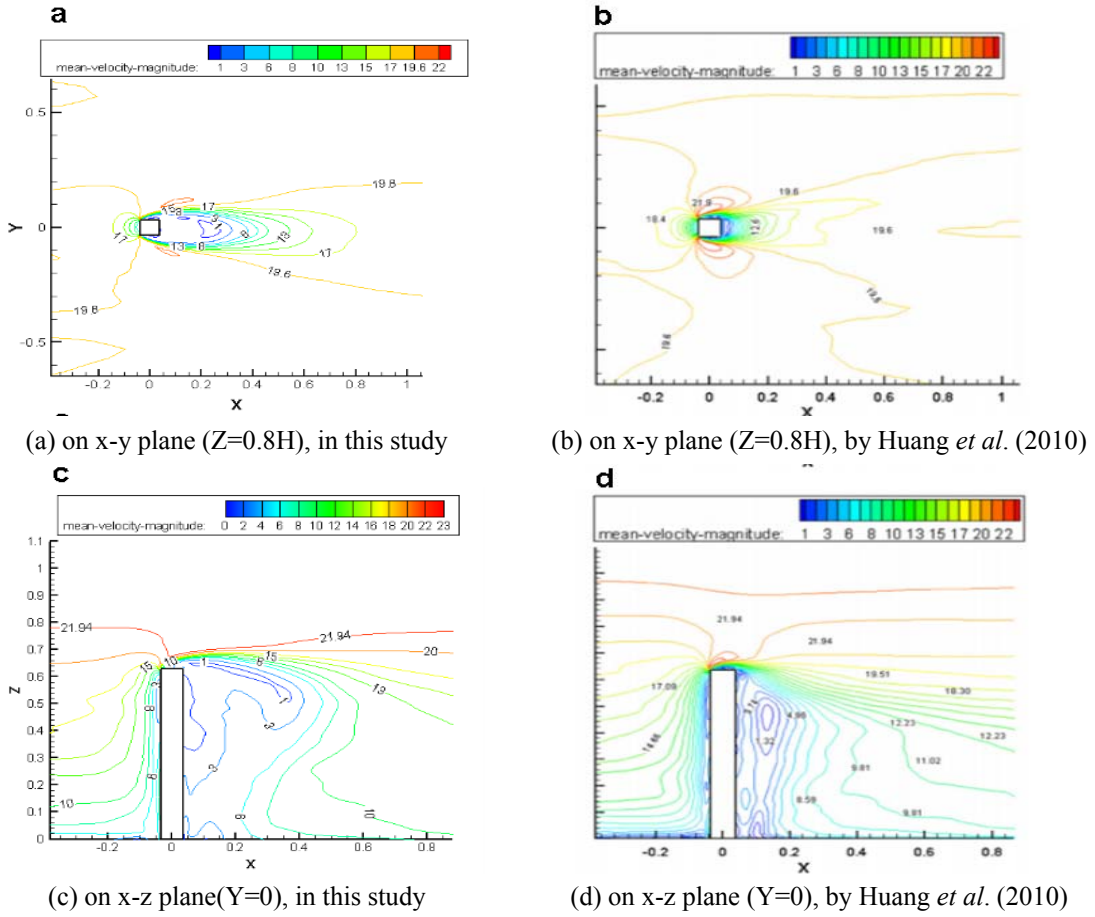


Fig. 3 Comparison of the mean velocity magnitude contour predicted by the DSRFG

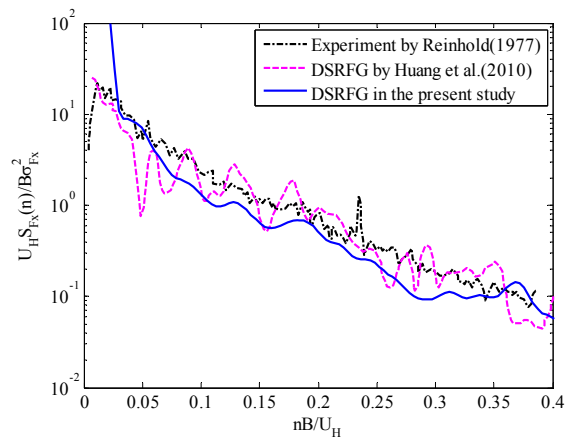
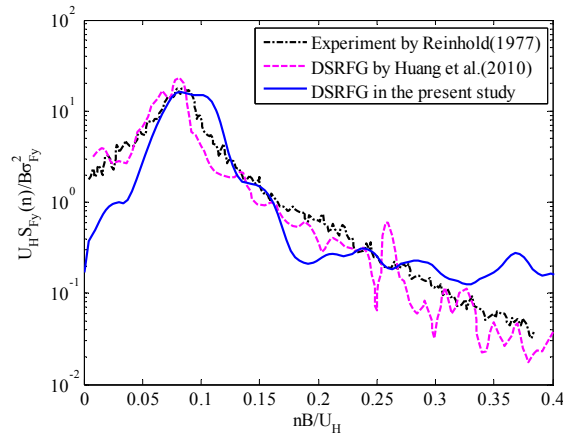
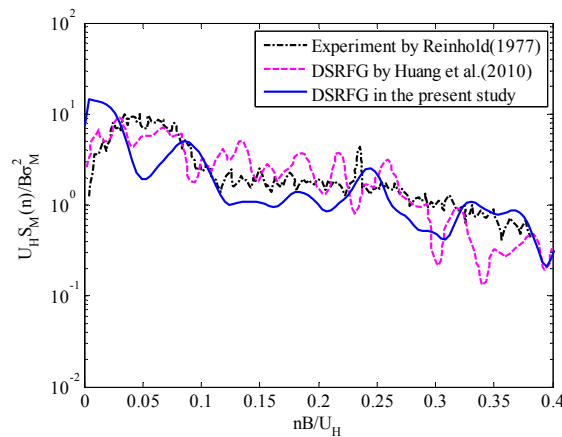


Fig. 4 Comparison of the along-wind force spectra at  $Z=0.8H$

Fig. 5 Comparison of the across-wind force spectra at  $Z=0.8H$ Fig. 6 Comparison of the torsional moment spectra at  $Z=0.8H$ 

### 3. Calculation setup

#### 3.1 Computational model

For studying the effects of turbulence characteristics on the wind-induced responses of tall buildings, a square building is adopted herein to represent a typical tall building. This square building is of a 50-storey steel structure with a cross-section area of  $40\text{ m} \times 40\text{ m}$  and  $200\text{ m}$  height. The typical Reynolds numbers involved in the simulations are in the range from  $2.7 \times 10^7$  (based on the width of the building) to  $1.35 \times 10^8$  (based on the height of the building). As shown in Fig. 9, the computational domain covers  $31B$  in the streamwise direction,  $14B$  in the spanwise direction and  $2H$  in the vertical direction. The total mesh number of the whole computational domain is approximate  $3.1 \times 10^6$ . The computational model of the tall building for the dynamic analysis is

simplified as a cantilever shear column with ten lumped masses; each lumped mass has two translational degrees of freedoms (DOFs) in horizontal directions (X and Y direction) and one rotational DOF in vertical (Z) direction, as shown in Fig. 7. The vertical distributions of the lumped mass, stiffness, moment of inertia and torsional stiffness of this building are also shown in Fig. 7. The natural frequencies and mode shapes of this tall building are shown in Fig. 8, while the damping ratio is assumed to be 1% for all the vibration modes (Wu *et al.* 2008).

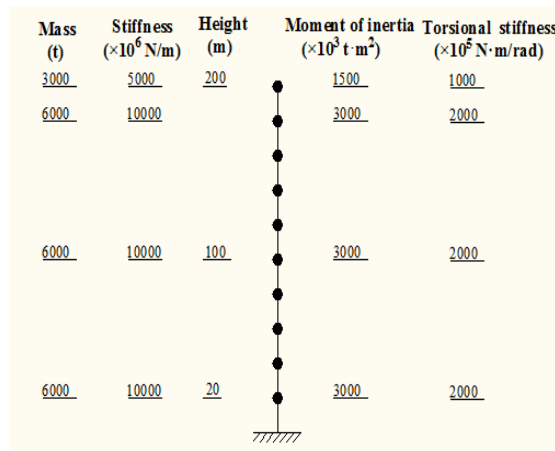


Fig. 7 Simplified computational model of the square tall building

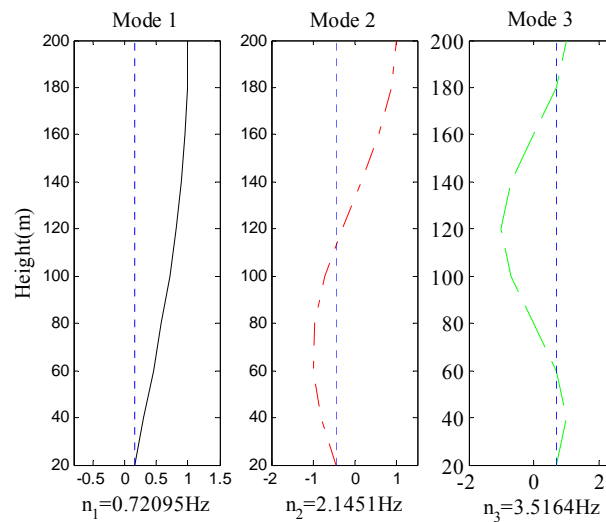


Fig. 8 Dynamic characteristics of the tall building

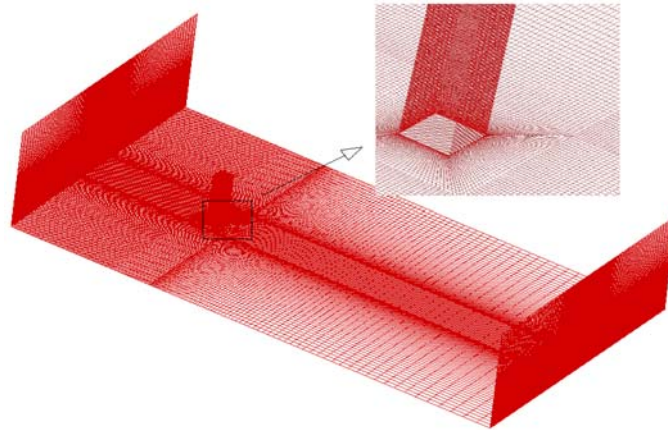


Fig. 9 Grid arrangement in the computational domain

### 3.2 Numerical setup in FLUENT

In this study, the numerical simulation is carried out by commercial software FLUENT while the inflow wind fields are generated by the DSRFG approach with the computer program made by the authors. The discretized equations are solved in a segregated manner with SIMPLC (Semi-Implicit Method for Pressure-linked Equations Consistent) algorithm. Second order discretization schemes are adopted for time and spatial discretization. The bounded central difference, a default convection scheme for LES in FLUENT, is used to discretize the convective terms of momentum equations for its relative low diffusivity. The second order backward difference is employed to discretize the time derivative. The Green-Gauss cell based method is used for numerical approximation of pressure gradients. A workstation with total 12 CPUs are used to carry out the present simulations. Considering the accuracy of the LES and computational cost, 0.01s per time step is adopt in the computations and the convergence criterion for the scaled residuals within each time step is less than 0.0001. The grid arrangement of the computational domain is shown in Fig. 9.

## 4. Effects of turbulent integral length scale on the wind-induced responses of a tall building

To investigate the influences of turbulence integral length scale on the wind-induced responses of the square tall building, five prescribed inflow conditions with different turbulence integral length scale values are generated using the DSRFG method. At six different heights in front of the building, time histories of the velocity components in the streamwise, spanwise and vertical directions were recorded. The five target profiles with different distributions of turbulence integral length scale are shown in Fig. 10 which displays that the turbulence integral scale values ascend with height and increase from case 1 to case 5. As shown in Fig. 11, the simulated velocity spectrum is in good agreement with the target von Karman spectrum. It is generally known that the change of turbulence integral length scale also represents the variations of spatial correlations of a

velocity field. As illustrated in Fig. 12, the correlation coefficients increased gradually from case 1 to case 5, which are consistent with the increments of the turbulence integral length scale.

To study the effects of turbulence integral length scale on the wind-induced response of the typical tall building, the profiles of the mean longitudinal wind speed and turbulence intensity of the incoming wind flow for the five different cases were identical. As shown in Figs. 13 and 14, the mean speed profiles and the turbulence intensity profiles were approximately the same for the different cases and consistent with the target profiles. From the instantaneous velocity field in the vertical plane shown in Fig. 15, it can be seen that the generated instantaneous velocity increased in vertical direction. Figs. 16 and 17 show the velocity magnitude contours in the vertical and horizontal directions, respectively. As shown in these figure, a number of eddies were generated by the DSRFG method and vortices were well produced in the separation region and in the wake flow.

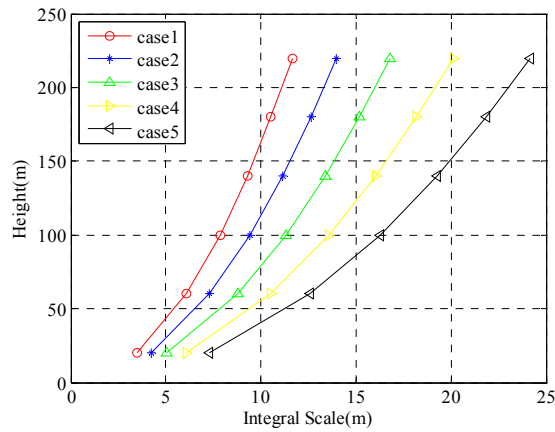


Fig. 10 The target turbulence integral length scale profiles for five cases

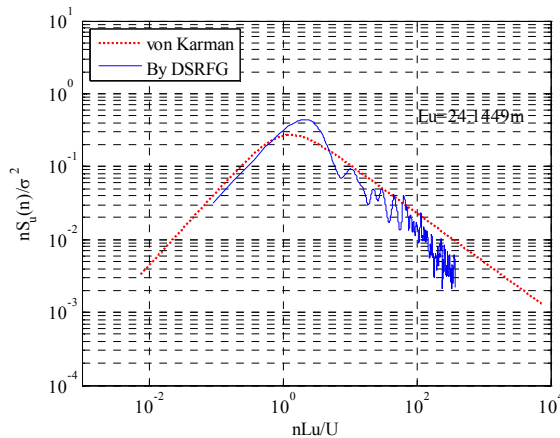


Fig. 11 Comparison of wind velocity spectra

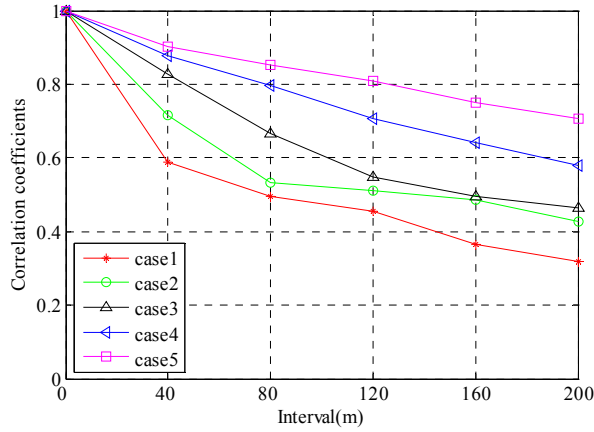


Fig. 12 Correlation coefficients of velocity at Z=20 m with other points along vertical direction

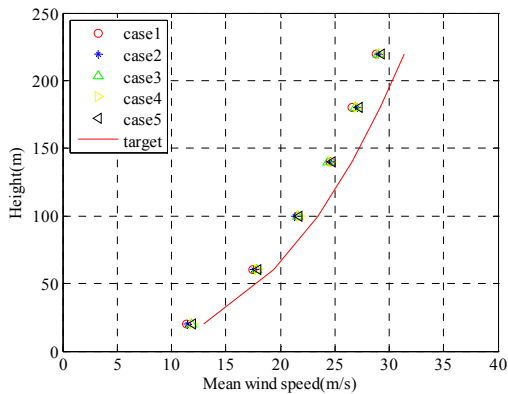


Fig. 13 mean wind velocity profiles for cases 1-5 and the target profile

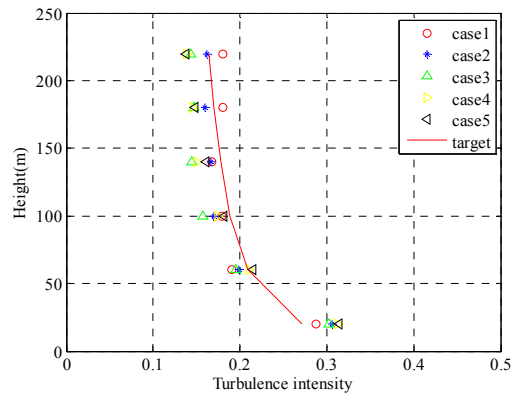


Fig. 14 Turbulence intensity profiles for cases 1-5 and the target profile

Along-wind forces, across-wind forces and torsional moments acting on the tall building were determined at ten different levels shown in Fig. 7 for the wind-induced response analysis. The spectra of the forces and the moment acting on the top lumped mass are shown in Fig. 18. The magnitudes of these spectra for cases 1-5 were comparable with each other, especially for the along-wind spectra. In the whole frequency range, the energy distributions were mostly consistent for the different cases while some discrepancies in certain frequency regions were observed. For the across-wind spectra, a typical peak around non-dimensional frequency of 0.11 was observed, which was induced by vortex shedding, as Strouhal number is about 0.12 for a square cylinder. Although the spectral shape patterns of the across-wind forces for the different cases were basically identical, the areas under the spectra were diverse with each other. Nevertheless, a uniform variation with the turbulence integral length scale could not be summed up. For the

torsional moments, the spectra also showed a peak at about non-dimensional frequency of 0.11, which revealed that vortex shedding also made contributions on the torsional moments. Actually, the characteristics of the spectra of the torsional moments are similar with those of the across-wind force spectra.

After obtaining the forces and torsional moments on the tall building, the structural responses were calculated by the *Newmark- $\beta$*  method. Owing to the space limitation of this paper, only time series of the acceleration responses atop the tall building are shown in Fig. 19. Comparisons of RMS of the responses of the tall building are presented in Fig. 20. It can be seen that for the along-wind responses including displacement, velocity and acceleration, the results for the five different cases were very close. For the across-wind responses, displacement and velocity responses keep consistent for cases 1-5. But it is hard to find a clear trend for the variation of the acceleration responses with the turbulence integral length scale. Similarly, the variation of the torsional responses with the turbulence integral length scale is also random.

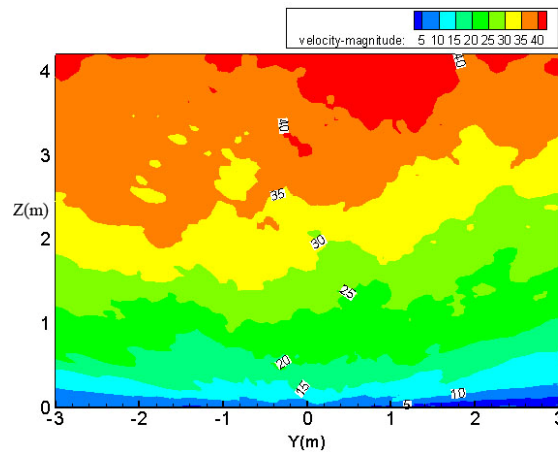


Fig. 15 Instantaneous velocity field at the inflow boundary

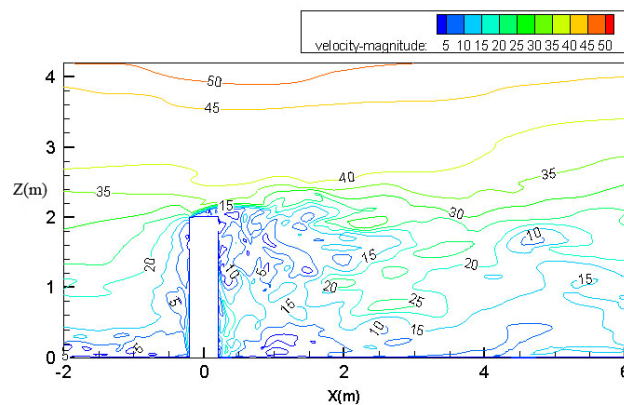


Fig. 16 Velocity magnitude contour of x-z plane ( $Y=0$ )

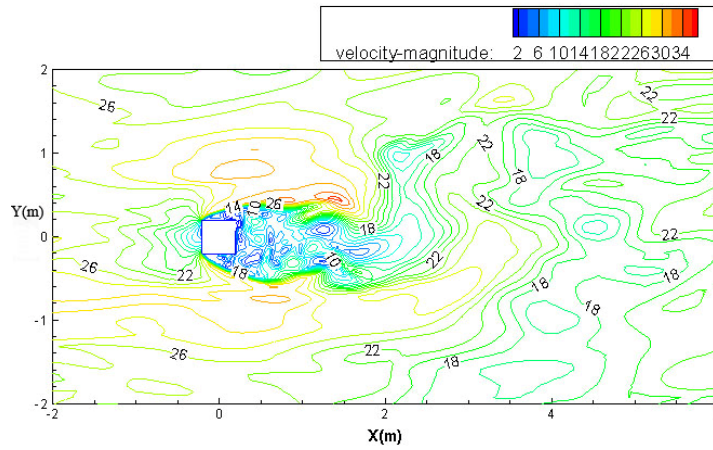
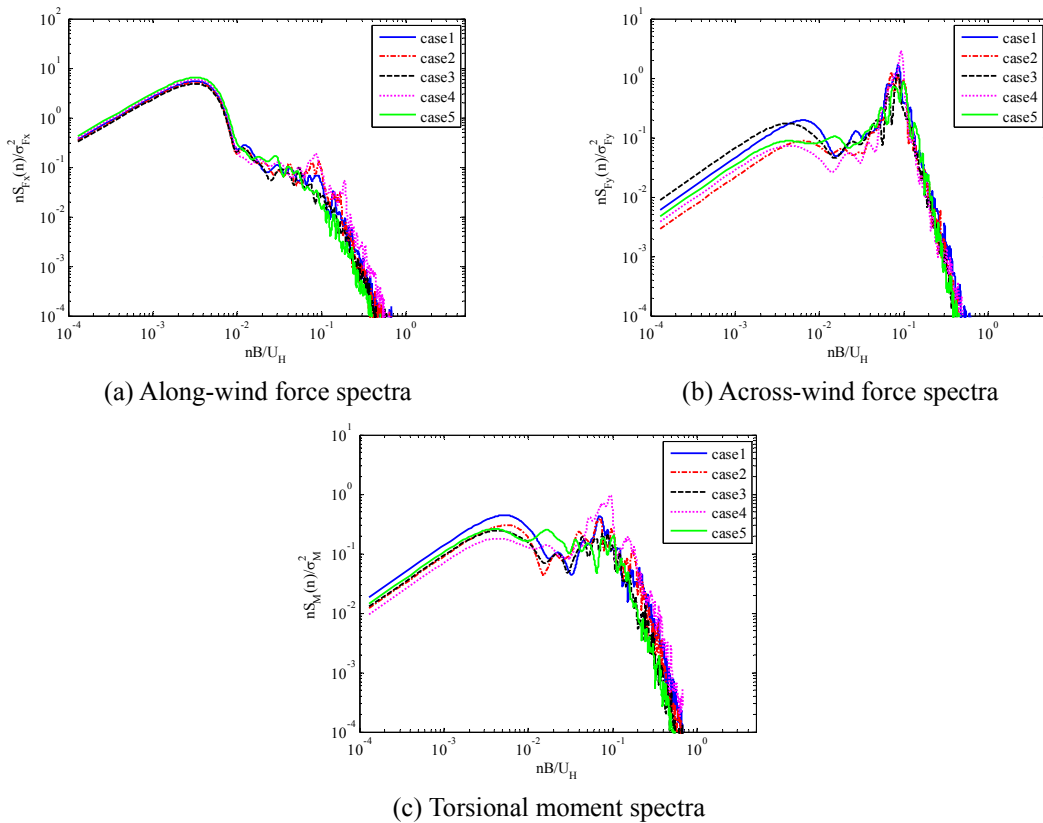


Fig. 17 Velocity magnitude contour of x-y plane (Z=150 m)



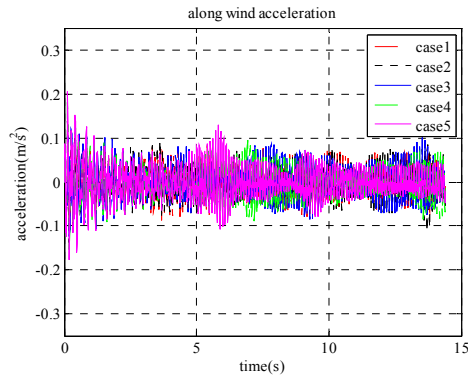
(a) Along-wind force spectra

(b) Cross-wind force spectra

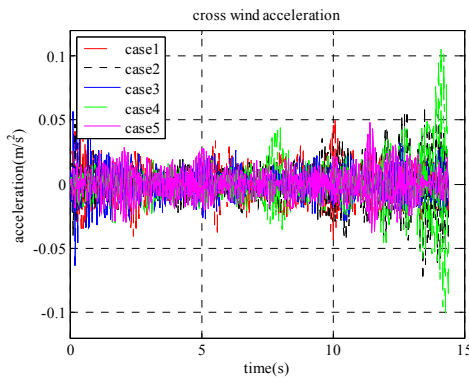
(c) Torsional moment spectra

Fig. 18 Spectra of the forces and torsional moment on the top lumped mass of the tall building

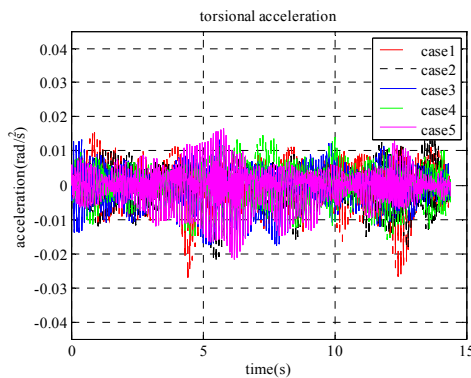
In summary, turbulence integral length scale did not show significant effects on the along-wind response. Negligible influences of the parameter were observed on the across-wind displacement and velocity responses. With the variation of turbulence integral length scale, the across-wind acceleration and torsional responses varied without a clear rule.



(a) Along-wind acceleration responses time series

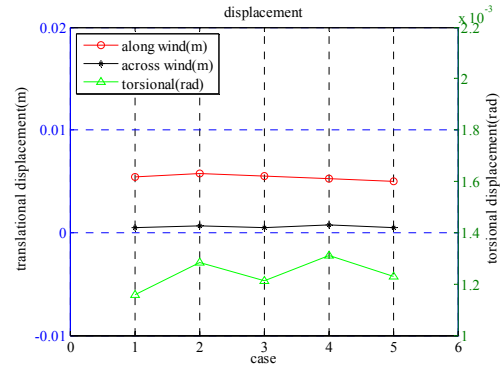


(b) Cross-wind acceleration responses time series

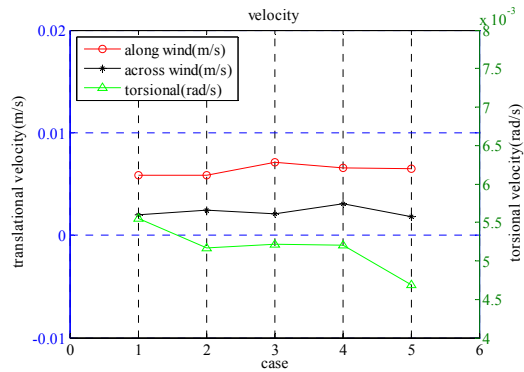


(c) Torsional acceleration responses time series

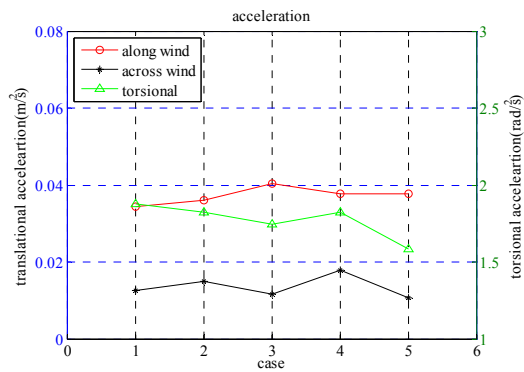
Fig. 19 Acceleration responses time series of the top lumped mass of the tall building



(a) RMS of displacement responses



(b) RMS of velocity responses



(c) RMS of acceleration responses

Fig. 20 Comparison of RMS of responses

### 5. Effects of turbulence intensity on the wind-induced responses

In order to study the effect of turbulence intensity on the wind-induced responses of the tall building, five flow fields with different turbulence intensity profiles were generated by the DSRFG approach. These five profiles are displayed in Fig. 21, which shows the vertical distributions of turbulence intensity at all heights increase from case 1 to case 5. Meanwhile, the other variables such as turbulence integral length scale and longitudinal wind speed for cases 1-5 are kept invariant to ensure the turbulence intensity to be the only variable. Fig. 22 shows the wind velocity spectra for cases 1-5 match well with each other, which means the flow fields of cases 1-5 have approximately the same value of the turbulence integral length scale. Meanwhile, evidence demonstrating this judgment is through the comparison of spatial correlations of wind velocities among these five cases as shown in Fig. 23. Good agreement of the correlation coefficients of velocity at  $Z=20$  m with those at other heights for cases 1-5 is observed in spite of some discrepancies at large intervals. The velocity profiles in Fig. 24 indicate the flow fields of cases 1-5 have the same vertical distribution of longitudinal wind speed.

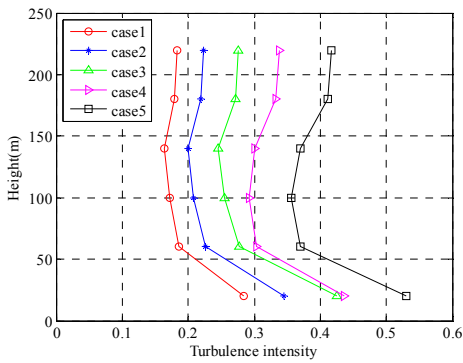


Fig. 21 Turbulence intensity profiles for cases 1-5

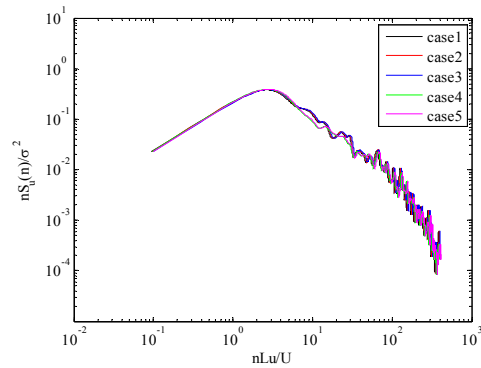


Fig. 22 Wind velocity spectra for cases 1-5

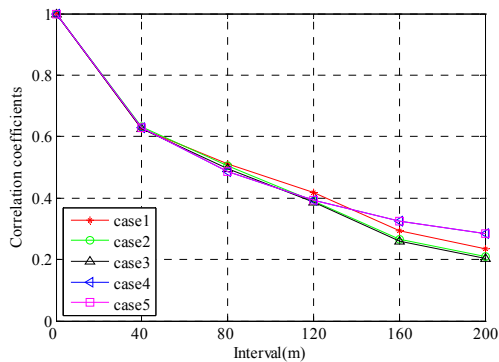


Fig. 23 Correlation coefficients of velocity at  $Z=20$  m with other points in the vertical direction

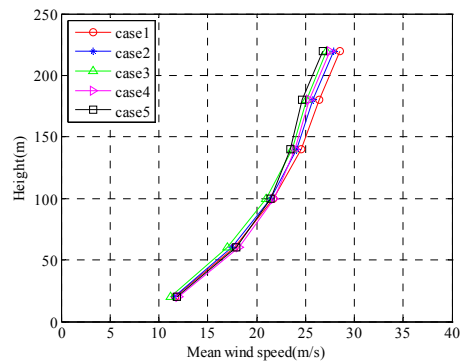


Fig. 24 Velocity profiles of cases 1-5

The spectra of the forces and torsional moment acting on the top lumped mass are shown in Fig. 25. For the along-wind force spectra, the magnitudes of the spectra and the areas under the spectra vary noticeably from case 1 to case 5, namely varying with the change of the turbulence intensity. The magnitudes and the areas decrease from case 1 to case 5 evidently. These changes reflect the variation of the aerodynamic drag force due to the variation of the turbulence intensity, which is consistent with the previous conclusion (Simiu *et al.* 1996). For the across-wind force spectra, the energy distributions are relatively more complicated compared with those of the along-wind force spectra. In the low frequency range, the areas under the spectra increase from case 1 to case 5. But around non-dimensional frequency of 0.11, the magnitudes of the spectra reduce with the growth of turbulence intensity, which can be explained by the observation made by Lee (1975a). His experiment showed the strength of the vortex shedding reduces as the growth of turbulence intensity. A typical peak around non-dimensional frequency of 0.11 is observed in all the across-wind force spectra and torsional moment spectra, which is induced by vortex shedding as Strouhal number is about 0.12 for a square cylinder.

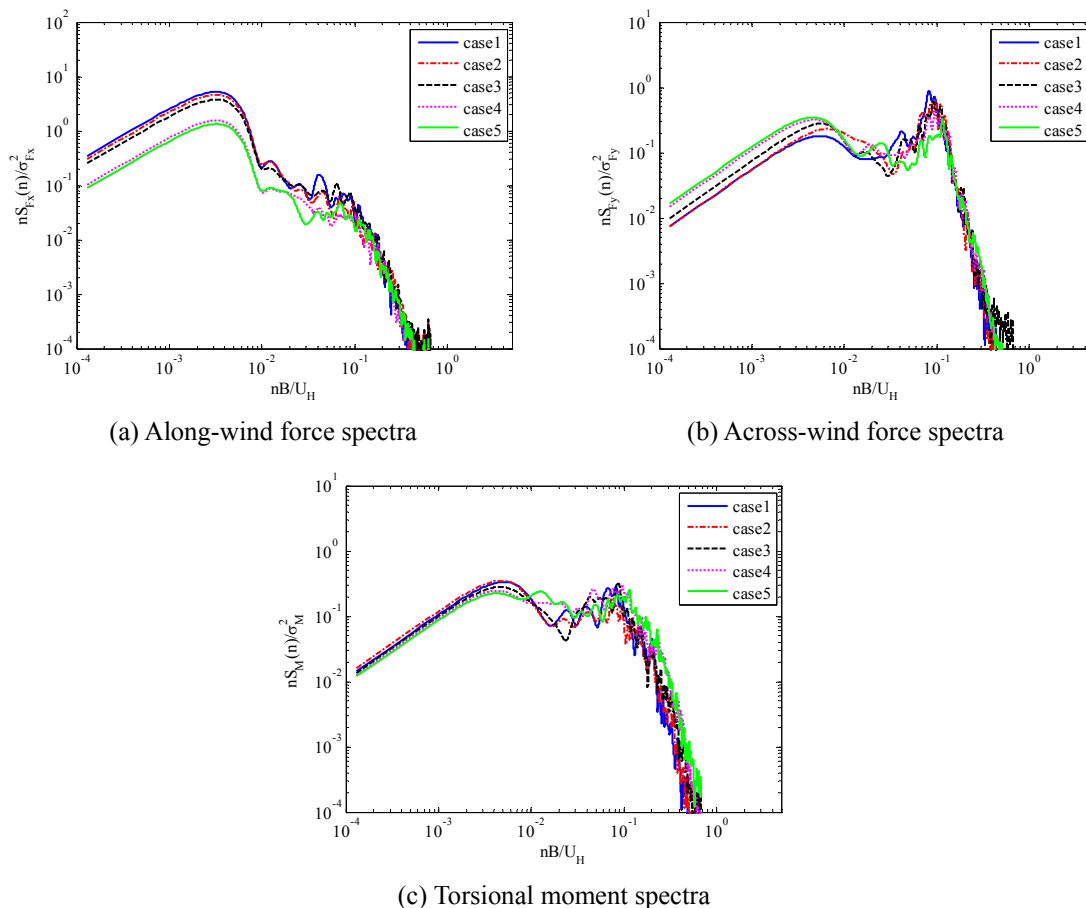
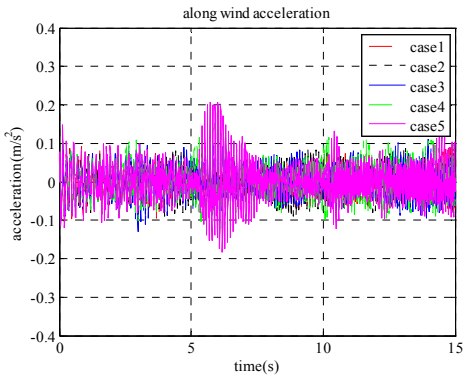
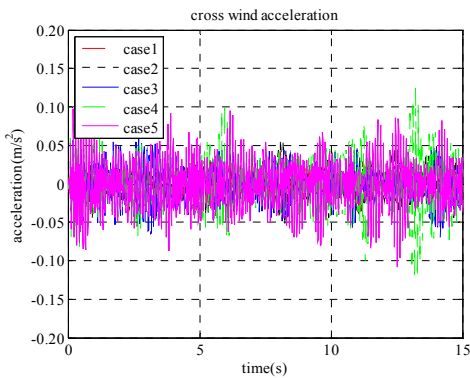


Fig. 25 Spectra of the forces and torsional moment on the top lumped mass of the tall building

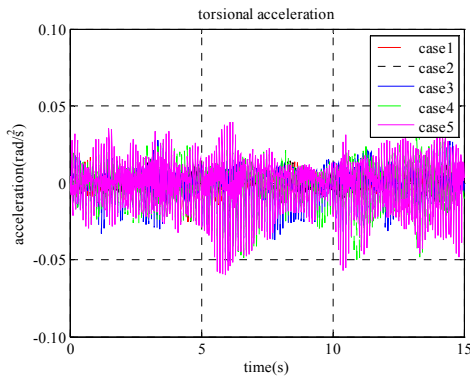
Fig. 26 presents the time series of the acceleration response of the top lumped mass. Comparisons of the RMS of the responses of the top lumped mass among the five cases are made in Fig. 27. For the displacement, the along-wind and torsional responses increase from case 1 to case 5 namely increasing with the growth of the turbulence intensity. Although the across-wind displacements also go up with the turbulence intensity, the growth magnitude is relatively small.



(a) Along-wind acceleration responses time series

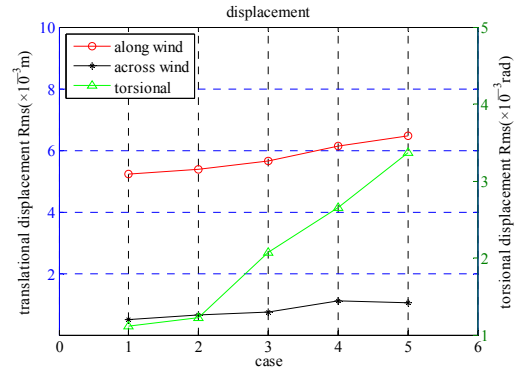


(b) Across-wind acceleration responses time series

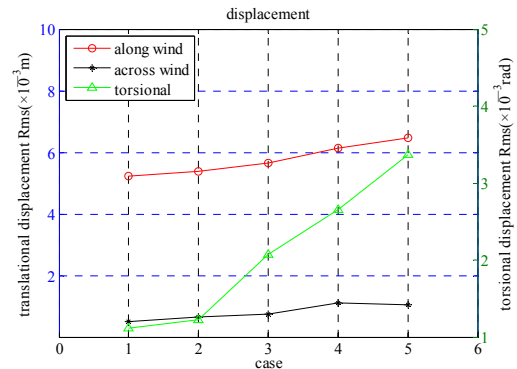


(c) Torsional acceleration responses time series

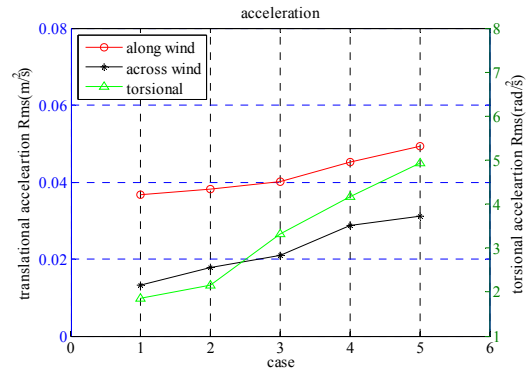
Fig. 26 Acceleration responses time series of the top lumped mass of the tall building



(a) RMS of displacement responses



(b) RMS of velocity responses



(c) RMS of acceleration responses

Fig. 27 Comparison of RMS of responses

For the velocity and acceleration responses, the responses in the three directions (along-wind, across-wind and torsion) all rise from case 1 to case 5. It means that the velocity and acceleration responses of the tall building in the three directions all increase with the turbulence intensity. So, it is concluded that turbulence intensity has significant effects on the wind-induced responses of the tall building.

## 6. Conclusions

The effects of free-stream turbulence on the wind-induced responses of a square tall building have been investigated by the LES with the DSRFG approach. It was found that turbulence intensity has significant effects on the wind-induced responses of the tall building. However, the effects of turbulence integral length scale on the wind-induced responses are not evident. Some conclusions from this study are summarized below.

- The DSRFG approach is able to produce turbulent wind flows obeying von Karman spectra with desired values of turbulence integral length scale. It can also generate turbulent wind flows satisfying the profiles of target turbulence intensity and mean wind speed. It is an effective tool to investigate the effects of turbulence characteristics on the wind effects on buildings and structures. Compared with wind tunnel testing, the LES with the DSRFG is higher-efficiency and easier to realize the target wind flow fields.
- Turbulence integral length scale did not have significant effect on the along-wind responses of the typical tall building. Negligible influence of the parameter on the across-wind displacement and velocity responses was observed. With the increase of turbulence integral length scale, the across-wind acceleration and torsional responses varied without a clear rule.
- For the displacements, the along-wind and torsional responses increased with the growth of turbulence intensity. Although the across-wind displacements also went up with turbulence intensity, the growth magnitude was relatively small. The velocity and acceleration responses of the tall building in the three directions all increased with turbulence intensity. So, it is concluded that turbulence intensity has significant effects on the wind-induced responses of the square tall building.

## Acknowledgments

The work described in this paper was fully supported by a grant from the Research Grants Council of Hong Kong Special Administrative Region, China (Project No: CityU 117709) and grants from the Natural Science Foundation of China (Project No: 51178179 and 91215302).

## References

- Braun, A.L. and Awruch, A.M. (2009), "Aerodynamic and aeroelastic analyses on the CAARC standard tall building model using numerical simulation", *Comput. Struct.*, **87**(9-10), 564-581.
- Hang, J. and Li, Y. (2012), "Macroscopic simulations of turbulent flows through high-rise building arrays using a porous turbulence model", *Build Environ.*, **49**, 41-54.
- Huang, M.F., Lau, I.W.H., Chan, C.M., Kwok, K.C.S. and Li, G. (2011), "A hybrid RANS and kinematic

- simulation of wind load effects on full-scale tall buildings”, *J. Wind Eng. Ind. Aerod.*, **99**(11), 1126-1138.
- Huang, S.H., Li, Q.S. and Xu, S. (2007), “Numerical evaluation of wind effects on a tall steel building by CFD”, *J. Constr. Steel Res.*, **63**(5), 612-627.
- Huang, S.H., Li, Q.S. and Wu, J.R. (2010), “A general inflow turbulence generator for large eddy simulation”, *J. Wind Eng. Ind. Aerod.*, **98**, 600-617.
- Huang, S.H. and Li, Q.S. (2010), “Large eddy simulation of wind effects on a super-tall building”, *Wind Struct.*, **13**(6), 557-580.
- Laneville, A. (1990), “Turbulence and blockage effects on two dimensional rectangular cylinders”, *J. Wind Eng. Ind. Aerod.*, **33**(1-2), 11-20.
- Lee, B.E. (1975a), “Some effects of turbulence scale on the mean forces on a bluff body”, *J. Wind Eng. Ind. Aerod.*, **1**, 361-370.
- Lee, B.E. (1975b), “The effect of turbulence on the surface pressure field of a square prism”, *J. Fluid Mech.*, **69**(2), 263-282.
- Li, C., Li, Q.S., Huang, S.H., Fu, J.Y. and Xiao, Y.Q. (2010), “Large eddy simulation of wind loads on a long-span spatial lattice roof”. *Wind Struct.*, **13**(1).
- Li, Q.S. and Melbourne, W.H. (1995), “An experimental investigation of the effects of free-stream turbulence on streamwise surface pressures in separated and reattaching flows”, *J. Wind Eng. Ind. Aerod.*, **51-52**, 313-323.
- Li, Q.S., Fang, J.Q., Jeary, A.P. and Wong, C.K. (1998), “Full scale measurements of wind effects on tall buildings”, *J. Wind Eng. Ind. Aerod.*, **74-76**, 741-750.
- Li, Q.S. and Melbourne, W.H. (1999a), “The effects of large scale turbulence on pressure fluctuations in separated and reattaching flows”, *J. Wind Eng. Ind. Aerod.*, **83**, 159-169.
- Li, Q.S. and Melbourne, W.H. (1999b), “Turbulence effects on surface pressures of rectangular cylinders”, *Wind Struct.*, **2**(4), 253-266.
- Li, Q.S., Wu, J.R., Liang, S.G., Xiao, Y.Q. and Wong, C.K. (2004a), “Full-scale measurements and numerical evaluation of wind-induced vibration of a 63-story reinforced concrete tall building”, *Eng. Struct.*, **26**(12), 1779-1794.
- Li, Q.S., Xiao, Y.Q., Wong, C.K. and Jeary, A.P. (2004b), “Field measurements of typhoon effects on a super tall building”, *Eng. Struct.*, **26**(2), 233-244.
- Lu, C.L., Li, Q.S., Huang, S.H., Chen, F.B. and Fu, X.Y. (2012), “Large eddy simulation of wind effects on a long-span complex roof structure”, *J. Wind Eng. Ind. Aerod.*, **100**(1), 1-18.
- Nakamura, Y. (1993), “Bluff-body aerodynamics and turbulence”, *J. Wind Eng. Ind. Aerod.*, **49**(1-3), 65-78.
- Reinhold, T.A. (1977), *Measurement of simultaneous fluctuating loads at multiple levels on a tall building in a simulated urban boundary layer*, Ph.D. Dissertation, Virginia Polytechnic Institute & State University, Virginia.
- Revuz, J., Hargreaves, D.M. and Owen, J.S. (2012), “On the domain size for the steady-state CFD modelling of a tall building”, *Wind Struct.*, **15**(4), 313-329.
- Saathoff, P.J. and Melbourne, W.H. (1987), “Freestream turbulence and wind tunnel blockage effects on streamwise surface pressures”, *J. Wind Eng. Ind. Aerod.*, **26**, 353-370.
- Saathoff, P.J. and Melbourne, W.H. (1989), “The generation of peak pressures in separated/reattaching flow”, *J. Wind Eng. Ind. Aerod.*, **32**, 121-134.
- Simiu, E. and Scanlan, R.H. (1996), *Wind effects on structures: fundamentals and applications to design*, John Wiley.
- Swaddiwudhipong, S. and Khan, M.S. (2002), “Dynamic response of wind-excited building using CFD”, *J. Sound Vib.*, **253**(4), 735-754.
- Tamura, T., Nozawa, K. and Kondo, K. (2008), “AIJ guide for numerical prediction of wind loads on buildings”, *J. Wind Eng. Ind. Aerod.*, **96**(11-12), 1974-1984.
- Tamura, T. (2009), “Large eddy simulation on building aerodynamics”, *Proceedings of the 7<sup>th</sup> Asia-Pacific Conference on Wind Engineering*, Taipei, Taiwan, November 8-12.
- Tieleman, H.W. and Akins, R.E. (1990), “Effects of incident turbulence on pressure distributions on rectangular prisms”, *J. Wind Eng. Ind. Aerod.*, **36**, 579-588.

- Tominaga, Y., Mochida, A., Murakami, S. and Sawaki, S. (2008), "Comparison of various revised k- $\epsilon$  models and LES applied to flow around a high-rise building model with 1:1:2 shape placed within the surface boundary layer", *J. Wind Eng. Ind. Aerod.*, **96**(4), 389-411.
- Varshney, K. and Poddar, K. (2011), *Experiments on integral length scale control in atmospheric boundary layer wind tunnel*, Springer Wien.
- Wu, J.R. Li, Q.S. and Tuan, A.Y. (2008), "Wind-induced lateral-torsional coupled responses of tall buildings", *Wind Struct.*, **11**(2), 153-178.
- Yahyai, M., Daryan, A.S., Ziaei, M. and Mirtaheri, S.M. (2011), "Wind effect on milad tower using computational fluid dynamics", *Struct. Des. Tall Spec.*, **20**(2), 177-189.
- Yoshida, M., Kondo, K. and Suzuki, M. (1992), "Fluctuating wind pressure measured with tubing system", *J. Wind Eng. Ind. Aerod.*, **42**(1-3), 987-998.

CC